Distance-based Neighborhood Scanning for Handover Purposes in Network with Small Cells

Michal Vondra, *Member, IEEE*, and Zdenek Becvar, *Member, IEEE*

Abstract—Deployment of small cells into existing mobile networks can improve throughput and users quality of service. However, the new tier composed of the small cells raises problems related to management of user's mobility. Moving users must be able to discover cells in their neighborhood. For this purpose, the users perform neighborhood scanning. The scanning process should be frequent enough to avoid situations when the user is not aware of a close cell as this one has not been scanned. However, the frequent scanning of a high number of neighboring cells leads to wasting battery of user equipments and to a reduction of user's throughput. Contrary, rare scanning can lead to a situation when a small cell is missing in the list of scanned cells and, thus, handover to it is not performed. It results in underutilization of the small cells and consequent overloading of macro cells. In this paper, we propose an efficient scanning algorithm suitable for future mobile networks. The objective of the proposed scheme is to maximize utilization of the small cells and to minimize energy consumption due to scanning. The proposal exploits graph theory to represent a principle of obstructed paths in combination with knowledge of previous visited cell and estimated distance between cells. As the results presented in the paper show, our algorithm reduces energy consumption due to scanning and enables higher exploitation of small cells by offloading macrocells.

Index Terms—*neighborhood scanning, handover, mobility prediction, small cells, heterogeneous networks, energy efficiency*

I. Introduction

DEPLOYMENT of small cells (SCeNBs) increases overall throughput of network and it enables to offload macro cells (MeNBs) [1]. On the other hand, a high number of SCeNBs in the network implies several problems. One of the major problems is related to mobility management [2]. If a user is moving, she/he must perform handover from a current serving cell to a target cell. To decide about proper time of handover, Reference Signal Received Power (RSRP) between a User Equipment (UE) and the serving and neighboring cells is measured. This process is known as neighborhood scanning.

The authors are with the Department of Telecommunication Engineering, Faculty of Electrical Engineering, Czech Technical University in Prague, Technicka 2, 166 27, Prague, Czech Republic. (e-mail: michal.vondra@fel.cvut.cz; zdenek.becvar@fel.cvut.cz).

Information about cells to which the handover can be performed from the current serving cell is stored by each base station in so-called Neighbor Relation Table (NRT) [3]. It means each cell in the network creates its own NRT containing all cells in its neighborhood. After the UE performs handover to the target cell, it receives a list of cells that should be scanned. This list, denoted as Neighbor Cell List (NCL), contains cells, which signal quality should be measured. The NCL includes cells operating in the same band as the serving one (intra-frequency) as well as those operating in a different bands (inter-frequency). The efficient scanning process can maximize utilization of SCeNBs and, consequently, higher Quality of Service (QoS) for users.

For scanning of the neighboring cells in LTE-A and WCDMA networks, so-called Automatic Neighbor Relation (ANR) [4] and Detected Set Reporting (DSR) [5] are defined by standards, respectively. By using these mechanisms, the UE needs not to know its neighboring cells before the scanning takes place since the UE can automatically scan only surrounding cells, which share the same frequency band as the serving cell [6], [7]. However, the major drawback of these mechanisms with respect to the future mobile networks considering carrier aggregation [8] or heterogeneity by means of multiple Radio Access Technology (RAT) consists in possibility of scanning only cells in the same band as the serving cell. Also, deployment of small cells in an orthogonal way, i.e., macro and small cells are not sharing the same bands, can lead to incomplete list of potential handover candidates. Efficient utilization of both ANR or DSR is not possible in these networks since the inter-frequency or inter-RAT cells cannot be discovered. To ensure inter-frequency and inter-RAT scanning, the serving cell has to inform the UEs about the bands or frequencies where potential neighboring cells can be discovered. If the inter-frequency and inter-RAT cells are not scanned, the cells using different frequency band or different RAT can be underutilized as those are not known to the UEs and handover to those cells cannot be initiated. Consequently, other cells can become overloaded.

On the other hand, if the UE scans an excessive number of neighboring cells, time for finding the most appropriate candidate for handover is significantly increased. It results in wasting battery power of the UE [9], reducing throughput of users, and lowering QoS due to more frequent occurrence of measurement gaps in data transmission [3]. In future mobile networks, dense deployment of small cells is assumed as a key enabler of 5G heterogeneous mobile networks. This may lead

to the scanning of a high number of cells if a large number of SCeNBs within a communication range of the MeNB is deployed. By using conventional methods for neighborhood scanning, all cells deployed in the range of MeNB are considered as regular neighbors of the MeNB. Therefore, all these cells should be scanned as potential handover candidates.

The contribution of this paper consists in proposal of the algorithm for neighborhood scanning, which focuses on minimization of the number of scanned cells and, therefore, on reduction of energy consumption of the UEs due to scanning if the UE is attached to the MeNB. At the same time, the proposed algorithm enables high utilization of the SCeNBs to maximize throughput of the UEs. This paper is an extension of our previous work [10], which exploits knowledge of previously visited cell and principle of obstructed paths from one cell to another. The extension with respect to our former work consists in consideration of relative distance among cells for scanning algorithm and its description by means of graph theory. This way, we postpone scanning until the UE becomes close to the area of potential handover. To that end, we define framework for distance estimation and we also analyze impact of relative distance inaccuracy together with inaccuracy of the UE speed estimation. Furthermore, definition of distance based scanning is provided including deep elaboration of self-configuration and scanning phases. Additional contribution comparing to our previous paper is evaluation of impact of the scanning algorithm on the energy consumption of UE and on the utilization SCeNBs by UEs. The algorithm is evaluated for OFDMA based LTE-A networks but it is generally applicable on all mobile networks including 5G.

The rest of this paper is structured as follows. Next section gives an overview on the state of art in area of neighborhood scanning in mobile networks. Section III thoroughly describes the principle of obstructed path and explains the proposed distance-based scanning algorithm. Then, Section IV describes distance-based scanning process including self-configuration phase. Simulation environment and parameters for performance evaluation are defined in Section V. In Section VI, competitive approaches are specified and simulation results to prove performance gain and robustness of the proposed solution are presented. The last section summarizes major conclusions and outlines potential future research directions.

II. RELATED WORKS

Most of recently described schemes for scanning considers scenarios with MeNBs only. However, application of these algorithms to the networks with SCeNBs leads to a significant increase in time required for neighborhood scanning. If the UE is connected to the SCeNB, the problem consists in discovering of all potential candidates for handover. This problem is addressed, for example, in [11], [12]. Both papers deal with a solution for minimization of so-called hidden node problem when two cells are neighbors but they are not able to receive signal of each other due to an obstacle between them (e.g., a wall). If the hidden cells are not discovered, they cannot be included in UE's NCL and handover to them is not possible. All discovered hidden nodes are included into NCL and treated in the same way as other cells in the NCL.

In case the UE is served by the MeNB, a large number of neighboring cells must be scanned if the SCeNBs underlying the MeNB are deployed densely. According to the schemes applied in 3GPP standard ([3] and [13]), the scanning process can be performed frequently only if RSRP of the serving cell is at a low level. However, the SCeNBs can be deployed also in areas with sufficient RSRP from the MeNB. Therefore, usage of this scheme would lead to the situation when the SCeNBs are not discovered. Consequently, main motivation for deployment of the SCeNBs, i.e., offloading of the MeNB and providing higher throughput to the UEs, is suppressed. Note that the simple solution by means of lowering the RSRP level for scanning of the SCeNBs would lead to redundant scanning and to consequent rise in energy consumption.

Another scanning algorithm is presented in [14] and proposed for 3GPP standard in [15]. The scheme is denoted as Background Inter-frequency Measurement (BIM) and it performs the scanning during the entire movement of the UE within area of the MeNB. To reduce amount of scanning events, the period for MeNB scanning is prolonged. This modification ensures lower power consumption and also keeps the possibility of finding a suitable SCeNBs for handover even if the RSRP of MeNB is sufficient. However, the proposed algorithm does not take into account impact of the density of SCeNBs on the optimum scanning period. It means the scanning period suitable for one MeNB with a given density of SCeNBs can lead to ignorance of the SCeNBs or to redundant scanning in another MeNB. Modification of the scanning interval of individual cells is exploited also in [16]. The authors suggest to select scanned cells according to the probability of handover to the given cell and SINR observed by the UE from its serving cell. In means more frequent handover targets are scanned more often than other cells. This leads to a significant reduction of the number of scanned cells while call drop rate is not impaired. However, like in the previous papers, the authors do not consider utilization of the SCeNBs and potential overloading of the MeNBs.

A scheme applicable for the scanning of SCeNBs within coverage of the MeNB is based on Radio-Frequency Fingerprints (RFFs). This method is investigated in [17], [18] and in [19]. By using this scheme, the UEs need to access a database with RFFs. On the basis of the RFF and measurement performed by the UE, an approximate position of the UE is determined. According to the observed position, potential handover candidates can be identified and scanned. This approach shows improvement in performance comparing to other approaches. However, its efficiency can be heavily impaired if deployment of cells or a channel quality are changed. It also implies high overhead due to a need for frequent exchange of the RFFs between location of the database and the UE if the database is deployed in the core network. If the database is deployed in the UE, then demands on the UE in terms of database storage rise significantly [20]. Especially in the network with small cells, the volume of

transferred and stored information is enormous and it can result in a reduction of QoS.

Approximate position and distance between the UE and femto cells is used in mechanism called Autonomous Search Function (ASF) [3], [21]. However, the scanning by using ASF is performed based on previously visited closed subscriber group member cells in whitelist. Therefore, the ASF is applicable for closed and hybrid femto cells only and it cannot be used for general small cells or femto cells with open access.

Another way of SCeNBs scanning is to take a mobility state of the UE into account. This possibility is investigated, for example, in [22] or [23]. According to [3], the mobility state is estimated based on the number of handovers performed within a specified time window. It enables to distinguish three mobility states: normal, medium, and high. Based on mobility state, the frequency of scanning is derived [14], [24].

With respect to above mentioned papers, our proposal reflects real speed of UEs as well as the relative position of UE in the network and aims on the efficient scanning process ensuring the best possible QoS while the energy consumption of the UEs due to scanning is minimized. The performance gain of our proposal is achieved by usage of the knowledge of previously visited cell, the principle of obstructed paths, and estimation of time of transition between cells.

III. PROPOSED DISTANCE-BASED ALGORITHM

This section provides description of the proposed distance-based algorithm. The proposed algorithm extends our work presented in [10] where we exploit knowledge of previous visited cell and principle of obstructed paths between two cells to reduce number of scanning events. In this paper, the proposed enhancement consists in consideration and derivation of the distance between neighboring cells. The algorithm targets especially NCL management for the UEs connected to the MeNBs (denoted as MUEs). The proposal can be also used for NCL management of UEs served by the SCeNBs (denoted as SCUEs). However, as it is explained later in this section, benefits for SCeNBs are limited due to the fact that case when the SCeNB covers several underlying SCeNBs is not expected to be often in real networks. Therefore we focus only on the NCL of MUEs.

To easy follow the proposal, we first define notation used in the paper and system model. Then, the principle of obstructed path combined with knowledge of previous visited cell is described. It is followed by description of the distance-based algorithm.

A. System model

To easily understand the proposal, notations used in this paper are summarized in Table I.

TABLE I
NOTATION USED FOR SYSTEM MODEL AND PROPOSED SCANNING ALGORITHM

Notation	Description
B_M / A_M	set of all cells to/from which the handover from/to $MeNB_M$ is possible
$cell_\alpha$ / $cell_\beta$	originating cell from which a UE can perform handover to $MeNB_M$ / destination cell to which a UE can perform handover from $MeNB_M$ ($cell_\alpha \in A_M$; $cell_\beta \in B_M$)
$p_{M\beta}$ / $p_{\alpha M}$	probability of handover from $MeNB_M$ to $cell_\beta$ / from $cell_\alpha$ to $MeNB_M$
$p_{\alpha M\beta}$	probability of handover from $MeNB_M$ to $cell_\beta$ after handover from $cell_\alpha$ to $MeNB_M$
B_{M_α}	set of distant neighbors of $cell_\alpha$ that can be reached through $MeNB_M$
$cell_x$ / $cell_y$	any cell within the $MeNB_M$ coverage ($cell_x$ / $cell_y \in (A_M \cup B_M)$)
v_{avg}	average speed of MUE computed after passing through the $MeNB_M$
$t_{\alpha M\beta}$	time between handover from $cell_\alpha$ to $MeNB_M$ and handover from $MeNB_M$ to $cell_\beta$
D_M / $d_{\alpha\beta}$	distance matrix of $MeNB_M$ containing the minimum distances between cells under coverage of the $MeNB_M$ / D_M contains elements $d_{\alpha\beta}$ expressing distance from $cell_\alpha$ to $cell_\beta$
$d_{\alpha\beta\_UE}$	distance from $cell_\alpha$ to $cell_\beta$ calculated by particular MUE
D_{M_α}	set of minimal distances between $cell_\alpha$ and distant neighbors of $cell_\alpha$ reachable through the $MeNB_M$
v_{est} / v_{real}	estimated speed of UE / real speed of UE
T_{M_α} / $t_{\alpha\beta}$	set of minimum time distances between $cell_\alpha$ and distant neighbors of $cell_\alpha$ reachable through the $MeNB_M$ / T_{M_α} contains elements $t_{\alpha\beta}$ expressing minimum time distance between $cell_\alpha$ and $cell_\beta$ reachable through the $MeNB_M$ calculated from estimated speed
$T_{M\_\alpha\_GI}$ / $t_{\alpha\beta\_GI}$	set of minimal distances expressed by means of time between $cell_\alpha$ and distant neighbors of $cell_\alpha$ reachable through the $MeNB_M$ considering the guard interval GI / element of set $T_{M\_\alpha\_GI}$
v'_{meas} / v'_{pre}	error in measurement of speed / error in speed estimation
v_{inac}	inaccuracy of speed determination ($= v'_{meas} + v'_{pre}$)
S_{MUE}	set of scanned cells defined for each MUE moving through the $MeNB_M$

The system model is described as follows. Let's assume N_{net} is the set of all cells (macro as well as small) in the network. The handover is performed at the edge of cells. In order to perform the handover from MeNB correctly, the NCL of MUEs should include all cells, to which the probability of handover from the serving $MeNB_M$ is higher than the threshold p_{thr}. The set B_M comprising all neighboring cells of the $MeNB_M$ is defined as:

$$B_M = \left\{ cell_\beta \in N_{net} \mid p_{M\beta} > p_{thr} \right\} \qquad (1)$$

where $p_{M\beta}$ is the probability of handover from the $MeNB_M$ to the neighboring cell $cell_\beta$. In real networks, the probability of handover $p_{M\beta}$ is observed by statistical evaluation of all previously performed handovers from the $MeNB_M$. The threshold p_{thr} must be adjusted for optimization of the performance [25]. With a higher value of the threshold, less neighboring cells are scanned and therefore, more potential handover candidates can be missed. Since our proposal aims on maximization of SCeNBs' utilization we set the threshold $p_{thr} = 0$.

Since the B_M contains all possible handover candidates of the $MeNB_M$, this set corresponds to the NRT in 3GPP. However, using all possible handover candidates for scanning is ineffective. Therefore, we derived the NCL for each MUE

using knowledge of the previous visited cell and available paths between cells as explained in the next subsection.

B. Principle of obstructed path and knowledge of previous visited cell

The number of scanned cells (included in B_M) when the UE is moving through the $MeNB_M$ can be reduced by using principle of obstructed path and knowledge of the cell visited before the $MeNB_M$ (denoted as previous visited cell).

Obstruction of the path between cells is phenomenon occurring if the cell with small coverage radius (e.g., SCeNB) is deployed within the radius of a large cell (e.g., MeNB). Without deployed SCeNBs, each user can pass from one side of the MeNB to another without handover. However, if the SCeNBs are deployed, the MeNB's cell overlaps with SCeNBs. When the SCeNB spans over the entire width of the street, the path is obstructed by this SCeNB. Thus, if the user is moving along this street, handover to the SCeNB is performed since the path is obstructed by this SCeNB. With increasing density of SCeNBs, more paths become obstructed from the MeNB point of view.

The principle of obstructed paths complemented with knowledge of the previous visited cell, labeled as $cell_\alpha$, enables to determine limited set of really accessible cells. At first, set of all potential previous visited cells has to be defined. This set, denoted as A_M, contains all cells from which the handover to the $MeNB_M$ is possible (note that this set do not need to be the same as set of B_M due to hysteresis for handover):

$$A_M = \left\{ cell_\alpha \in N_{net} \mid p_{\alpha M} > p_{thr} \right\} \qquad (2)$$

where $p_{\alpha M}$ represents the probability of handover from the $cell_\alpha$ to the $MeNB_M$.

By exploiting the knowledge of the previous visited $cell_\alpha$ and the principle of obstructed path, particular $cell_\alpha$ is known after handover to $MeNB_M$ is performed and the set B_M can be narrowed down to the set B_{M_α} defined by the subsequent formula:

$$B_{M\_\alpha} = \left\{ cell_\beta \in B_M \mid \left(p_{\alpha M\beta} > p_{thr} \right) \wedge \left(cell_\alpha \in A_M \right) \right\} \qquad (3)$$

where $p_{\alpha M\beta}$ represents the probability of handover from the $MeNB_M$ to the $cell_\beta$ if the user comes to the $MeNB_M$ from the particular $cell_\alpha$. In other words, the set B_{M_α} contains all cells, which can be reached from the $MeNB_M$ if the MUE's last visited cell was $cell_\alpha$. This set of cells is denoted as distant neighbor cells (DNCs) of the $cell_\alpha$. The NCL of MUE can be reduced only to the cells included in the set B_{M_α} after the handover from the $cell_\alpha$ to the $MeNB_M$ is performed. Note that the set B_{M_α} includes also $cell_\alpha$, since the MUE can turn and go back to the $cell_\alpha$ any time. Also note that not only SCeNBs but also MeNBs can be included in both A_M and B_M. As can be seen from (3), the B_{M_α} is always subset of the B_M, i.e., $B_{M\_\alpha} \subseteq B_M$.

Benefits of the principle of obstructed path and of the knowledge of previous visited cell can be demonstrated by example shown in Fig. 1. In a conventional way, the MUE has to scan 10 neighboring cells (9 SCeNBs + 1 MeNB) belonging to B_2 during the movement of the MUE within the area of MeNB$_2$. Contrary, if the proposed approach is considered, the MUE scans only 4 neighboring cells (i.e. SCeNB$_{13}$, SCeNB$_{10}$, SCeNB$_{15}$, and SCeNB$_{14}$) belonging to B_{2_14} after the MUE leaves SCeNB$_{14}$ and attaches to the MeNB$_2$.
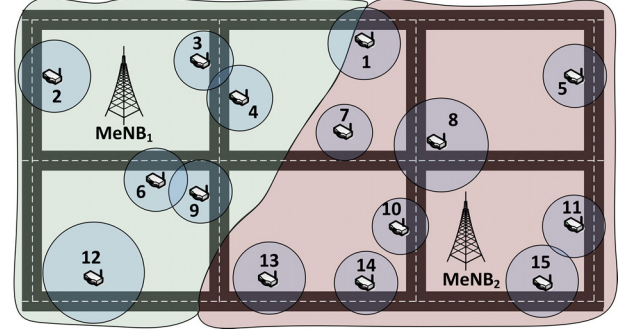

Fig. 1. Example of network deployment.

For the expression of the DNC relations among all cells within the $MeNB_M$ coverage, we adopt the graph theory. For each $MeNB_M$ in the network, the graph $G_M(V_M, E_M)$ is defined. The set of vertices (V_M) of the graph G_M represents all cells from which the handover to the $MeNB_M$ is possible or to which the handover from the $MeNB_M$ is possible (i.e., $A_M \cup B_M$). The set of edges (E_M) of the graph shows the links between DNCs. The degree of any vertex x denoted as $d(v_x)$ implies the number of DNCs and therefore the number of cells that need to be scanned by the MUE after performing handover from a general $cell_x$ to the $MeNB_M$ (i.e., in case that the $cell_x$ becomes the previous visited cell $cell_\alpha$).

The example in Fig. 1 can be interpreted by two graphs as shown in Fig. 2. For the clarity of graph expression, the edges from any vertex x to the same vertex (i.e., v_x, v_x) corresponding to cases when $cell_\beta = cell_\alpha$ are not depicted in Fig. 2 as this path is applicable for all cells (as explained above). We assume handover at the edge of cells in our example. Thus, if handover from any $cell_x$ to the $MeNB_M$ and then to any $cell_y$ is possible (i.e., $cell_y$ is DNC of $cell_x$), the handover from $cell_y$ to the $MeNB_M$ and then to the $cell_x$ is also possible. However in real network (and as well in our simulations), hysteresis is exploited to avoid redundant handovers. Consequently, the DNC relations may not be reciprocal.
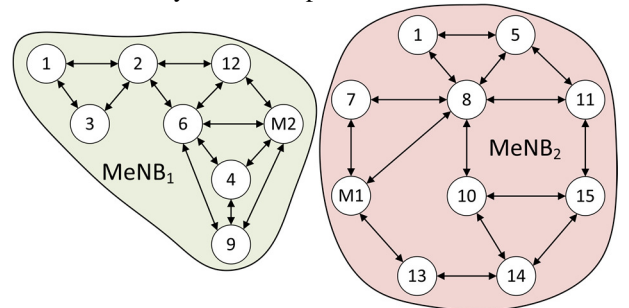

Fig. 2. Expression of distant neighbor cell relations by graph theory.

The examples in Fig. 1 and Fig. 2 show few typical cases, which can occur in the network. The first case is the direct neighborhood of two cells, e.g., $SCeNB_3$ and $SCeNB_4$ in Fig. 1. Users passing from the $SCeNB_3$ to the $SCeNB_4$ do not pass through $MeNB_1$. Therefore, these two cells are not the DNCs and consequently, the cells are not interconnected by edge in Fig. 2. Of course, both SCeNBs must be included in their own NRT so they are aware of each other.

Another situation appears when two cells are the direct neighbors as well as the DNCs. It means handover directly between two cells as well as the handover through the MeNB is possible. In Fig. 1, this case is represented, e.g., by $SCeNB_6$ and $SCeNB_9$. From the $MeNB_1$ point of view, these two cells are regular DNCs. Thus this relation is represented by edge in Fig. 2.

Analogical case is that the SCeNB obstructs only a part of the road as, e.g., $SCeNB_7$. When the UE leaves, for example, $SCeNB_8$, it is possible to bypass the $SCeNB_7$ and enter directly the $MeNB_1$. In this case, all the DNCs of the $SCeNB_7$ are also the DNCs of each other among themselves. This is again reflected by edges between the $MeNB_1$ and the $SCeNB_8$ in Fig. 2. Note that if the SCeNB spans over more MeNBs (such as the $SCeNB_1$ in our example), then it is included in all G_M belonging to all MeNBs, which overlap with the SCeNB.

The proposed algorithm is designed for creation of the NCL of MUE. However, it can be used also for the NCL of SCUE. Nevertheless, the SCeNBs are of a limited range and the obstructed paths are not so frequent under coverage of the SCeNBs. Thus, the NCL of SCUE composed according to our proposal (set B_{M_α}) is usually identical with the set B_M (NRT of SCeNB).

The drawback of the principle of obstructed paths is that during the whole movement of MUEs through the MeNB, the MUE have to scan all cells included in the B_{M_α} no matter what is the distance between the MUE and the DNC. Therefore, we further propose to exploit an estimation of the distances between the $cell_\alpha$ and the $cell_\beta$ and between the $cell_\alpha$ and the MUE. This allows a reduction in the number of cells in the NCL by exclusion of cells, which cannot be accessed right now due to user's location.

C. Weighted graph for definition of relation between DNCs

The main problem related to the determination of the distance between two cells and among the cells and the UE consists in accuracy of localization of the user and the SCeNBs. Localization by using information from the network (e.g., Angle of Arrival, Time of Arrival, etc.) or satellite navigation systems (e.g., GPS, GLONASS, etc.) can be very inaccurate in urban areas or even impossible indoor due to unavailable signal. Another problem of these techniques is relatively high energy consumption if those systems are integrated in mobile devices such as smart phones [26].

In terms of SCeNB, the location of micro and pico cells is usually known very precisely as those are deployed by operators. However, localization accuracy of femto cells is limited since the femto cells are deployed by the users.

Moreover, user's movement is restricted to street or maps with a certain level of volatility. Therefore, the determination of mutual distance among SCeNBs and among SCeNBs and users based on real position is not applicable globally. To enable utilization of the proposal in general scenario when the position of objects is not known accurately, we focus on exploitation of only relative distance. To determine the relative positions of the cells, we use the statistical observation of users' movements. The relative position of the cells is determined based on the user's average speed v_{avg} and time $t_{\alpha M\beta}$ that the MUE spends connected to the MeNB when passes from $cell_\alpha$ to $cell_\beta$.

The relative distance is represented in graphs, based on Fig. 2, by weighted edges as depicted in Fig. 3. Individual neighbors of the MeNB are represented in the graph by vertexes and weights assigned to the edges. The weights represent the shortest distance between two cells. Note that the distances from $cell_x$ to the $cell_y$ is the same as distance from $cell_y$ to the $cell_x$ if no hysteresis for handover is considered (as presented in Fig. 3 for clarity purposes). However, in real network as well as in our simulation, the hysteresis is included. Hence, the distances between cells can be different for opposite directions.
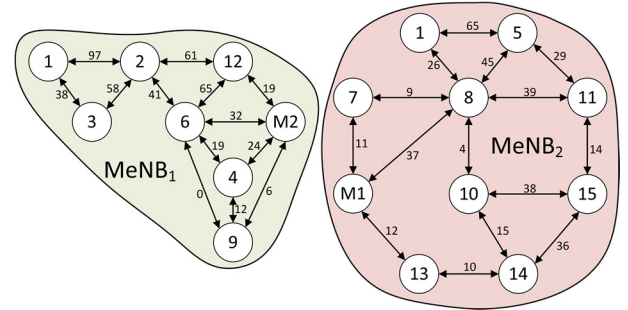

Fig. 3. Expression of example network deployment by graph theory with weighted edges.

Evaluation of edges can be described for each MeNB by a distance matrix D. For the $MeNB_M$, the distance matrix D_M is defined as:

$$D_M = \begin{pmatrix} d_{11} & \cdots & d_{1\beta} & \cdots & d_{1m} \\ \vdots & \ddots & \vdots & \cdot^{\cdot^{\cdot}} & \vdots \\ d_{\alpha 1} & \cdots & d_{\alpha\beta} & \cdots & d_{\alpha m} \\ \vdots & \cdot^{\cdot^{\cdot}} & \vdots & \ddots & \vdots \\ d_{n\beta} & \cdots & d_{n\beta} & \cdots & d_{nm} \end{pmatrix} \qquad (4)$$

where $\alpha = \{1, 2\ldots, n\}$ and $n = |A_M|$ is the total number of cells from which handover to the $MeNB_M$ can be performed; similarly $\beta = \{1, 2\ldots, m\}$ where $m = |B_M|$ is the total number of cells to which the handover from the $MeNB_M$ can be performed; and $d_{\alpha\beta}$ is the shortest observed distance between the $cell_\alpha$ and the $cell_\beta$. Note that the distance $d_{\alpha\beta}$ may not be the same as distance $d_{\beta\alpha}$.

In general, the distance $d_{\alpha\beta}$ is calculated as:

$$d_{\alpha\beta} = v_{avg} \cdot t_{\alpha M\beta} \qquad (5)$$

where $t_{\alpha M \beta}$ is the time spent by the MUE connected to the $MeNB_M$ when the MUE passes from the $cell_\alpha$ to the $cell_\beta$; and v_{avg} represents the average speed of the MUE during movement from the $cell_\alpha$ to the $cell_\beta$. The $t_{\alpha M \beta}$ can be expressed as difference between the handover from the $cell_\alpha$ to the $MeNB_M$ ($t_{\alpha M}$) and the time instant of the handover from the $MeNB_M$ to the $cell_\beta$ ($t_{M\beta}$), i.e., $t_{\alpha M \beta} = t_{M\beta} - t_{\alpha M}$.

The main challenge of the proposed algorithm is the detection of the UE's speed and the estimation of the speed for future movement in the MeNB as it influences efficiency of scanning. For low speed users (pedestrians), we can exploit algorithm of speed estimation based on correlation coefficients of OFDM system as described in [27], further analyzed in [28] for indoor and outdoor environment. In addition, the algorithm is experimentally validated for indoor environment in [29]. This algorithm shows average error of speed estimation less than 3 % [28] for outdoor pedestrians, which is more than sufficient for our algorithm. The speed estimation can be used for users (both pedestrians as well as vehicular) moving at a speed up to 4 m/s [27]. For users moving at a speed higher than 4 m/s, we assume usage of navigation systems, such as GPS, with even more precise speed estimation. Therefore, the speed estimation exploited in our paper represents the worst case scenario. In addition, we also investigate impact of the speed determination inaccuracy on the performance of the proposed NCL scanning algorithm later in the paper.

IV. DISTANCE-BASED SCANNING

To facilitate implementation of the proposed scanning to real networks, the self-configuration phase of the algorithm has to be completed before scanning process itself. Distance-based self-configuration phase is outlined in the following subsection. In the second subsection, process of the distance-based scanning (DBS) is described.

A. Self-configuration for distance-based scanning

The first step after the new MeNB is deployed is self-configuration phase. At the beginning of this phase, the D_M is empty and DNCs of the $MeNB_M$ are not known. The elements of the D_M are set in the following way:

$$d_{\alpha\beta} = \begin{cases} 0 & for \quad \alpha = \beta \\ \infty & otherwise \end{cases}$$

Note that the $d_{\alpha\beta}$ if $\alpha = \beta$ is kept equal to zero all the time as the MUE can turn back anytime and this time cannot be estimated. This, on one hand, lowers efficiency of our proposal in terms of the number of scanned cells, but on the other hand, it avoids missing cell in the NCL.

The self–configuration phase is depicted in Fig. 4. After each handover to the $MeNB_M$, the timer t_M is launched and previously visited cell $cell_\alpha$ is stored. During the MUE's connection to the $MeNB_M$ in self-configuration phase, the MUEs scan all cells included in NRT with a scanning period of Δt. At the beginning, the NRT can be derived from approximate network information together with sensing

algorithm, such as in [30].

As long as the MUE is connected to the $MeNB_M$ the speed of user is measured periodically using algorithms defined in [29] or global navigation systems for users indoor and outdoor, respectively. When the handover from the $MeNB_M$ to the $cell_\beta$ is performed, the timer t_M is frozen and its value is stored in $t_{\alpha M \beta}$. The distance $d_{\alpha\beta\_UE}$ between $cell_\alpha$ and $cell_\beta$ is calculated according to (5) by using time $t_{\alpha M \beta}$ together with v_{avg} measured by the UE. The derived $d_{\alpha\beta\_UE}$ is then compared with $d_{\alpha\beta}$ already stored in D_M. If the new calculated value of $d_{\alpha\beta\_UE}$ is lower than the former $d_{\alpha\beta}$, the $d_{\alpha\beta}$ is replaced by $d_{\alpha\beta\_UE}$ so that:

$$d_{\alpha\beta} = min\left(d_{\alpha\beta}, d_{\alpha\beta\_UE}\right) \qquad (6)$$

After performing a sufficient number of handovers, the distance matrix D_M is filled by the shortest distances between distant neighbors and the self-configuration phase is completed. Remaining infinite values of some elements $d_{\alpha\beta}$ indicate that the $cell_\beta$ is not the distant neighbor of $cell_\alpha$, thus transition from the $cell_\alpha$ to the $cell_\beta$ through the $MeNB_M$ is not possible. It means the path between these two cells is obstructed.
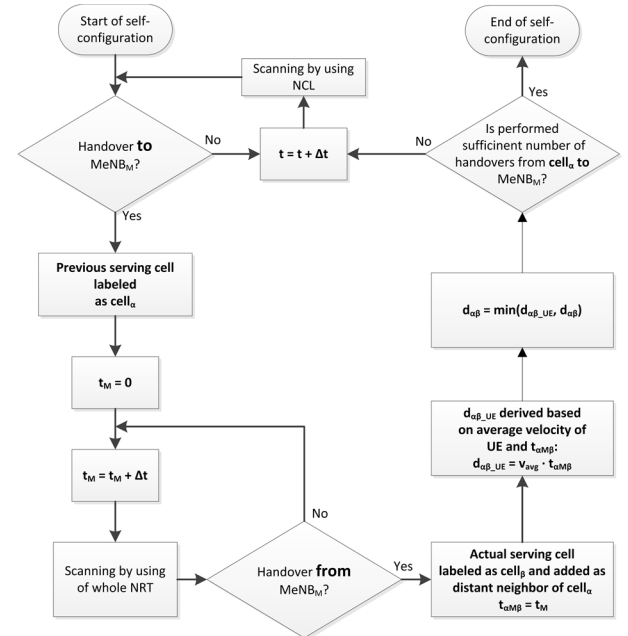

Fig. 4. Proposal of self–configuration.

Note that the impact of duration of the self-configuration phase has been already investigated in our previous work [10]. Based on the results, the duration of self-configuration depends on the number of handovers performed to the new installed $MeNB_M$. Although the duration of self-configuration is longer in comparison to conventional algorithms, we have to keep in mind that the self-configuration phase for the $MeNB_M$ is required only once after its first deployment. If any change in neighborhood of the new $MeNB_M$ occurs (for example, a new cell is inserted to the network or a cell is

turned off or moved) the $MeNB_M$ is able to react and adapt to this change in self–optimization phase during normal operational state as follows. After plugging any new cell (MeNB or SCeNB) to the vicinity of $MeNB_M$, this new cell is added as the DNC of all cells within the $MeNB_M$ range. It means new cell is added to each row of the D_M with value of $d_{\alpha\beta}$ set to 0. If (3) is not fulfilled after a given number of handovers, $d_{\alpha\beta}$ is set to ∞ and this new cell is not considered for scanning by the UEs entering the $MeNB_M$ from the $cell_\alpha$. Analogically, the new cell is included as a new row in the D_M of the $MeNB_M$ and elements $d_{\alpha\beta}$ are set to ∞ if (3) is not fulfilled after the predefined number of handovers. If (3) is fulfilled, $d_{\alpha\beta}$ is set according to (5).

After finishing the self-configuration phase, the set of cells for scanning is further managed during DBS.

B. Distance-based scanning process

After finishing the self-configuration, the row α of the D_M contains the shortest distances from the $cell_\alpha$ to all neighboring cells of the $MeNB_M$. All cells with finite distance are considered to be the DNCs of the $cell_\alpha$ and those are included in the set D_{M_α}:

$$D_{M\_\alpha} = \left\{ d_{\alpha\beta} \in D_M \mid d_{\alpha\beta} < \infty \right\} \tag{7}$$

If the UE performs handover from the $cell_\alpha$ to the $MeNB_M$, the set D_{M_α} is sent to the UE by the $MeNB_M$. This set represents the list of all cells suitable for the handover denoted as NCL. The NCL also contains the information on the shortest distance to particular neighboring cell. Note that the NCL itself is transmitted also for common approaches. Thus this does not imply any additional signaling. The only additional overhead is introduced by information on the shortest distance between cells. This leads to overhead of several bits (e.g., 10 bits per one neighboring cell from D_{M_α} enables reporting of distance up to 1023 m with accuracy of 1 m) required for the NCL distribution to the UE after the UE enters the $MeNB_M$. Therefore, the additional overhead can be neglected. Moreover, by reduction of the number of scanning events with respect to existing approaches, the overall overhead due to the scanning can be even lowered by our proposal.

After each handover to the $MeNB_M$, the timer t_M in MUE is launched. Also, the speed of UE is estimated (v_{est}) based on the current and previous speed. For the sake of simplicity, we assume only simple linear extrapolation for the speed prediction, i.e.:

$$v_{est}(s) = \frac{1}{p} \sum_{i=1}^{p} v(s-i) \tag{8}$$

where $v_{est}(s)$ is the future estimated speed and p is the number of previous steps taken into account (for our evaluation, ten samples are considered). Based on the MUE's estimated speed v_{est}, the MUE recalculates the distances $d_{\alpha\beta}$ (in the set D_{M_α}) to

the minimum time $t_{\alpha\beta}$ (in the set T_{M_α}) that is needed to reach individual distant neighbors. The $t_{\alpha\beta}$ is computed in the following way:

$$t_{\alpha\beta} = \frac{d_{\alpha\beta}}{v_{est}} \tag{9}$$

The v_{est} is only a prediction of real average speed v_{real} in the future. Thus, the v_{est} is affected by the error in speed measurement (v'_{meas}) and error in estimation of the future speed (v'_{pre}). The v_{est} is the sum of the real speed and both errors:

$$v_{est} = v_{real} + v_{inac} = v_{real} + v'_{meas} + v'_{pre} \tag{10}$$

Exact determination of v_{real} in the time of handover to the MeNB is not realistic and we can assume that $v_{est} \neq v_{real}$. In case the estimated speed $v_{est} < v_{real}$, all minimal achievable time $t_{\alpha\beta}$ (calculated according to (9)) are higher than the real one. This may cause that the MUE arrives to the vicinity of $cell_\beta$ before the scanning of this cell is initiated. Then, user cannot connect to the $cell_\beta$ and the SCeNBs are underutilized. Contrary, when $v_{est} > v_{real}$, the minimal time $t_{\alpha\beta}$ is lower than the real time spent under $MeNB_M$. Due to the shorter minimal time $t_{\alpha\beta}$, the scanning of neighboring cell is performed too early and can be considered as redundant. From the above two options, the second alternative is acceptable as early scanning does not result into significant decrease in QoS while efficient offloading of the MeNBs by SCeNBs is ensured. To avoid underestimation of v_{est}, we consider a Guard Interval (GI) which decreases $t_{\alpha\beta}$, derived by (9), to $t_{\alpha\beta\_GI}$. Thus, all elements $t_{\alpha\beta}$ from the set T_{M_α} are recalculated to set of minimum times $T_{M\_\alpha\_GI}$ as follows:

$$t_{\alpha\beta\_GI} = t_{\alpha\beta} - GI \tag{11}$$

Usage of the GI ensures that the cells are scanned with a sufficient time reserve before handover and a deterioration of QoS is suppressed. Impact of the GI on the performance is evaluated in the paper.

The main idea of our proposal consists in the fact that during the movement through the $MeNB_M$, the MUE scans only the neighboring cells, which are in proximity of the MUE and which are really accessible. It means the MUE scans only cells with minimal achievable time $t_{\alpha\beta}$ lower than elapsed time t_M spent by the UE in the $MeNB_M$. Therefore, the final set of scanned cells can be expressed as follows:

$$S_{MUE} = \left\{ t_{\alpha\beta\_GI} \in T_{M\_\alpha\_GI} \mid t_{\alpha\beta\_GI} < t_M \right\} \tag{12}$$

The proposed algorithm for selection of cells to be scanned is summarized in Fig. 5.
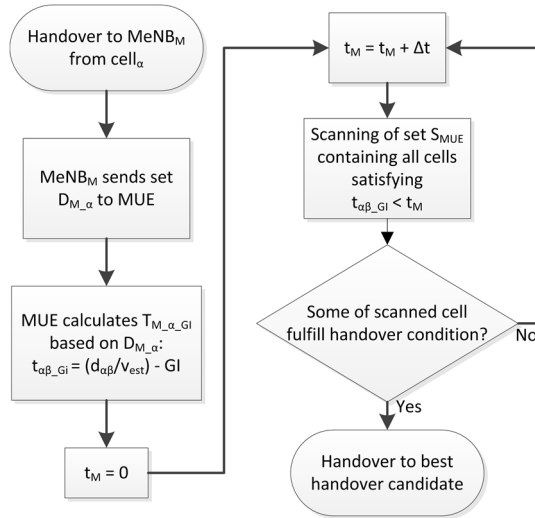
Fig. 5. Derivation of set of cells to be scanned.

Note that the D_M is continuously managed and updated in the same way as in self-configuration phase during self-optimization phase. It means values of elements $d_{\alpha\beta}$ in D_M are modified if a shorter path is found.

V. SIMULATION MODEL AND SCENARIO

We assess the proposed algorithm by simulations in MATLAB. As a simulation environment, a part of Prague, Czech Republic is chosen. In Fig. 6, simulation area with twelve blocks of buildings with different number of floors is shown. Among those blocks, apartments, offices, restaurants, and working places are distributed. In the simulation area, four fixed MeNBs providing LTE-A coverage are placed according to the real location of Vodafone MeNBs. The SCeNBs (represented by femto cells) are dropped at random place and random floors in each block. The position of femto cells is randomly generated in every simulation drop. In total, ten drops with a length of 500 000 steps are run. We assume the SCeNBs and the MeNBs do not use the same frequencies.

Fig. 6. Environment for simulation with depicted position of MeNBs (blue circle) and SCeNBs (orange cross).

Signal propagation is derived in line with the recommendations of Small Cell Forum. For signal attenuation from the MeNBs and the SCeNBs, Okumura-Hata [31] and ITU-R P.1238 [32] path loss models are used, respectively.

There are 100 UEs moving in the simulation area. The movement of those UEs is based on Manhattan mobility

model with Points of Interests (POIs) using graph theory approach as described in [16]. The model in [16] assumes constant speed of users. For our algorithms, the speed can influence the performance significantly. Therefore, we enhance original mobility model by acceleration distribution as presented in [33]. The distribution of user's speed as well as the distribution of acceleration is normal with mean value 1.127 m/s [33]. We consider pedestrians in the simulations. The reason is that the movement of pedestrians is of more degrees of freedom comparing to movement of vehicular users as the pedestrians are not limited only by streets. Therefore, pedestrians represent the worst case for our proposed scanning algorithm. Estimation of users' speed is performed based on [27], [28], and [29]. According to the [28], we assume maximum estimation error of 3 % in general scenario but we also investigate the impact of estimation error beyond this limit later in the paper.

Based on the maximum speed of users in simulation and based on [15], the default scanning period Δt is set to 1 second. Default value of *GI* used for our proposal is set to 1 second.

Major simulation parameters are listed in Table II.

TABLE II
SIMULATION PARAMETERS

Parameter	Value
Carrier frequency [GHz]	2
Transmitting power of MeNB / SCeNB [dBm]	27 / 15
Height of MeNBs / SCeNBs / UEs [m]	32 / {1.5 + 3×(floor−1)} / 1.5
Number of MeNBs / SCeNBs / UEs	4/ {0 −200} / 100
Attenuation of walls [dB]	10
Hysteresis for handover [dB]	4
Mean speed of users [m/s]	1.127 [33]
Standard deviation of speed [m/s]	0.5324 [33]
Mean acceleration [m/s^2]	0.0004 [33]
Standard deviation of acceleration [m/s^2]	0.2175 [33]
Maximum speed of user [m/s]	2.4999 [33]
Default accuracy of speed estimation [%]	3 [28]
Energy consumption per scanned cell, ρ [mWs]	3 [14]
Default scanning period, Δt [s]	1
Default Guard Interval, GI [s]	1
Step of simulation [s]	1
Total time of simulation, T_{SIM} [s]	500 000
Number of simulation drops	10

VI. PERFORMANCE EVALUATION

In this section, the performance of our algorithm is compared with competitive algorithms. The section is divided into three subsections. In the first subsection, competitive algorithms are described. Then, performance metrics are introduced. In the last subsection, simulation results are presented and discussed.

A. Competitive algorithms

Three algorithms are compared with our proposal: Mobility State Estimation-Based Scanning (MSE-BS) [14]; Background Inter-frequency Measurement (BIM) [13], [14]; Obstructed Path (OP) algorithm [10]. Note that we have compared our algorithm also with handover history [34] and with sensing algorithm [30] in our former paper. However, for the sake of

clarity, we do not present those algorithms here as our former proposal outperforms all of them as shown in [10].

First of the compared algorithm, MSE-BS, performs scanning based on the mobility state of the UE [14]. This algorithm selects the cell for scanning based the mobility state. Consequently, only the UEs in the normal state perform scanning of the SCeNBs. In our simulations, all UEs are in the normal mobility state as those can fully exploit advantages of the SCeNBs [3]. Therefore, all UEs perform scanning of neighboring cells with an interval of 1 second. With respect to the system model described in section III.A, all cells included in B_M (see (1)) are scanned.

The second algorithm, BIM, prolongs the scanning period in order to save energy. The prolongation depends on required savings of energy consumption. The scanning is done over the set B_M, however, the scanning interval is changing depending of required energy consumption. In our evaluations, we consider scanning periods $\Delta t = 2, 5, 10,$ and 20 seconds.

Last, the performance is also compared with the OP algorithm. In this case, only really accessible cells are scanned. Those cells are included in the set B_{M_α} (3).

The proposed distance-based scanning, denoted as DBS, scans only cells included in S_{UE} defined by (12).

B. Performance metrics

All algorithms are compared by means of average number of scanned cells, prolongation of time in MeNB, utilization of SCeNBs and energy efficiency of scanning.

The average number of scanned cells is expressed as:

$$N_{avg}^{a\lg} = \frac{\sum_{k=1}^{u} N_k^{a\lg}}{\sum_{k=1}^{u} T_{M\_k}^{a\lg} \cdot \Delta t} \tag{13}$$

where u is the total number of UEs in simulation, Δt is the scanning period, $T_{M\_k}^{a\lg}$ is the total time spent by the k-th UE connected to the MeNBs if scanning algorithm alg is used, and $N_k^{a\lg}$ is the number of scans performed by the k-th MUE connected to the MeNB during the simulation.

The prolongation of time in MeNBs can be described as follows:

$$\eta_{\Delta t} = \frac{\sum_{k=1}^{u} T_{M\_k}^{BIM_{\Delta t}} - \sum_{k=1}^{u} T_{M\_k}^{\min}}{\sum_{k=1}^{u} T_{M\_k}^{\min}} \cdot 100\% \tag{14}$$

where $T_{M\_k}^{BIM_{\Delta t}}$ is the total time spent by the k-th UE in the MeNBs for BIM algorithm by using scanning interval Δt and $T_{M\_k}^{\min}$ is the minimum time spent by the k-th UE in the MeNBs by using $\Delta t = 1$ s (i.e., by using other compared algorithms).

Utilization of the SCeNB is defined by the next formula:

$$\mu_{\Delta t} = 100 - \left(\frac{\sum_{k=1}^{u} T_{SC\_k}^{\max} - \sum_{k=1}^{u} T_{SC\_k}^{BIM_{\Delta t}}}{\sum_{k=1}^{u} T_{SC\_k}^{\max}} \cdot 100\% \right) \tag{15}$$

where $T_{SC\_k}^{BIM_{\Delta t}}$ is the total time spent by the k-th UE in the MeNBs for BIM algorithm by using scanning interval Δt and $T_{SC\_k}^{\max}$ is the maximum time spent by the k-th UE in the MeNBs by using $\Delta t = 1$ s (i.e., by using other compared algorithms).

Another compared aspect is the energy consumption due to scanning. The average energy consumption is linearly dependent on the number of scanned cells [14]. Therefore, it is defined as:

$$E_{avg}^{a\lg} = N_{avg}^{a\lg} \cdot \rho = \frac{\sum_{k=1}^{u} N_k^{a\lg}}{\sum_{k=1}^{u} T_{M\_k}^{a\lg} \cdot \Delta t} \cdot \rho \tag{16}$$

where ρ means the average energy consumption per one scanning of one cell. According to the [14], ρ is set to 3 mWs.

C. Simulation results

In this section, the results of simulations are presented to provide comparison of the performance with respect to the competitive approaches.

Fig. 7 shows the average number of scanned cells per second when the UE is connected to the MeNBs. As can be seen, the MSE-BS algorithm introduces the highest amount of scanning event out of all compared algorithms for all densities of SCeNBs. This algorithm scans all cells to which the handover from MeNBs is possible. Therefore, the number of scanned cells rises with the number of SCeNBs. The BIM algorithm reaches lower average number of scanned cells than the MSE-BS. The number of scanned cells decreases with prolongation of Δt. For example, prolongation of Δt from 10 to 20 s leads to reduction in the average number of scanned cells per second from 2 to 1. However, as in case of the MSE-BS, the number of scanned cells is rising with the density of deployment of SCeNBs. Therefore, the usability of this algorithm is limited by density of SCeNBs.

Contrary to the BIM and MSE-BS, the number of scanned cells is not rising continuously with the density of SCeNBs for the OP and for the proposed DBS. For low density of SCeNBs, the number of scanned cells rises with the number of cells. Then, the average number of scanned cells reaches its maximum (at roughly 20 SCeNBs) and decreases for higher density of SCeNBs. The reason is that the paths among cells become more and more obstructed for higher amount of SCeNBs. Thus, the number of real neighboring cells is getting lower. Note that the proposed DBS outperforms the OP by up to 50 % (the average number of scanned cells is reduced from 6 to 3 for 20 SCeNBs). From Fig. 7 can be also seen that the DBS algorithm reaches similar results as the BIM with $\Delta t = 2$ s and BIM with $\Delta t = 10$ s for lower and higher densities of
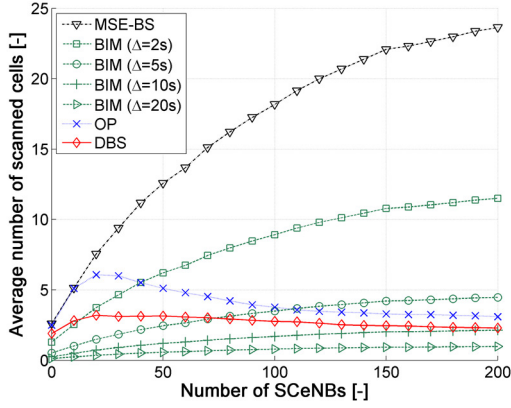
This article has been accepted for publication in a future issue of this journal, but has not been fully edited. Content may change prior to final publication. Citation information: DOI 10.1109/TVT.2015.2402753, IEEE Transactions on Vehicular Technology

> REPLACE THIS LINE WITH YOUR PAPER IDENTIFICATION NUMBER (DOUBLE-CLICK HERE TO EDIT) <　　10

SCeNBs, respectively.

Fig. 7.　Average number of scanned cells (N_{avg}^{alg}) over density of SCeNBs.

As can be seen in Fig. 7, the lowest number of scanned cells can be reached by the BIM with long Δt. However, a prolongation of the Δt can lead to the prolongation of the time spent by the UE connected to the MeNB as the neighboring cells cannot be discovered by the UE and handover cannot be performed. A prolongation of the time in MeNBs subsequently leads to the underutilization of the SCeNBs. Therefore, we analyze impact of the prolongation of Δt on the prolongation of the time in MeNBs and the utilization of SCeNBs.

The prolongation of Δt is used only by the BIM algorithm. All other algorithms perform scanning regularly every second (shown by red curve in Fig. 8 and in Fig. 9). By using $\Delta t = 1$ s, the prolongation of the time in MeNB is negligible and the users stay minimum time connected to the MeNBs. Contrary, using longer Δt leads to more time spent by the UEs attached to the MeNB. The time in MeNB rises also with the density of SCeNBs. For 200 SCeNBs and $\Delta t = 20$ s, the time in MeNB is prolonged for more than 16 %.
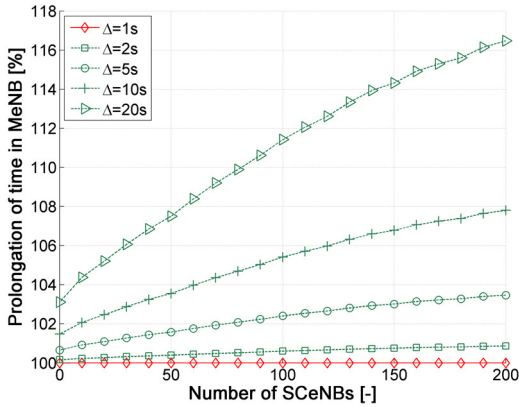

Fig. 8.　Prolongation of time spent by UEs connected to the MeNBs ($\eta_{\Delta t}$).

The prolongation of the time of connection to MeNB leads, at the same time, to a shortening of the time of connection to the SCeNBs. The main purpose of the SCeNBs in network is to improve QoS for users in its proximity. Therefore, lowering utilization of the SCeNBs leads to a loss in their potential to improve network performance. The utilization of SCeNBs in dependence on the scanning period for different densities is depicted in Fig. 9. This figure shows the most notable underutilization of SCeNBs for $\Delta t = 20$ s and for low densities of SCeNBs. In case of five SCeNBs in scenario, its potential is exploited only at 63.5 %. It means more than one third of capacity of the SCeNBs is not utilized, since the UE is not able to discover the SCeNBs in time. With rising density of the SCeNBs, their utilization rises. Note that sum of the $\eta_{\Delta t}$ and $\mu_{\Delta t}$ is not equal to 100 % since the absolute values of time spent by the UEs in the MeNBs and SCeNBs are different and both are related to $T_{M\_k}^{\min}$ and $T_{SC\_k}^{\max}$.
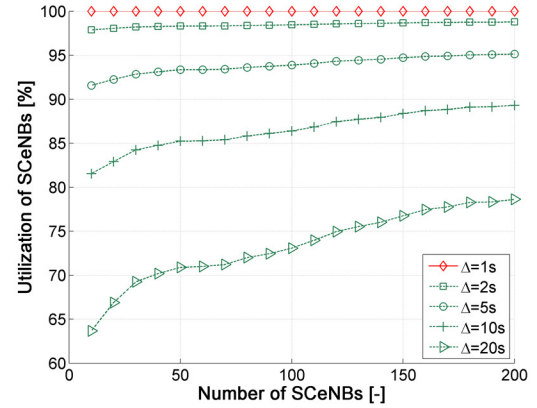

Fig. 9.　Impact of density of small cells and scanning interval (Δt) on utilization of SCeNBs ($\mu_{\Delta t}$).

In Fig. 10, the average energy consumption per second caused by scanning is presented. Fig. 10a shows comparison of all algorithms while Fig. 10b depicts zoom for algorithms showing low energy consumption. For deeper comparison, we implemented the prolongation of scanning period (Δt) also for our proposed DBS.

As can be seen, the highest energy consumption is reached, as expected, by the MSE-BS algorithm. For 200 SCeNBs, the average energy consumption per second is more than 70 mWs. If the same Δt is used by the BIM and our proposed scheme, the energy consumption is reduced for up to 85 % (for $\Delta t = 2$ s and 200 SCeNBs).

Comparing the DBS with $\Delta t = 1$ s with our previous proposal (OP algorithm [10]), the energy consumption is significantly reduced for all densities of SCeNBs. The reduction is lowered for more than 60 % for most of the densities (except very low density).
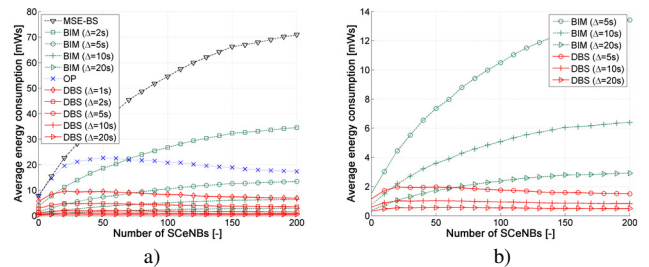

Fig. 10.　Average energy consumption due to neighborhood scanning, E_{avg}^{alg}, (a) and detailed comparison of energy consumption for the most energy efficient algorithms (b).

Furthermore, impact of the *GI* on performance of the proposed algorithm is shown in Fig. 11. The prolongation of the time in MeNB due to the late scanning of neighboring cell is depicted over the variance of inaccuracy of speed determination v_{inac}. The results for scanning periods $\Delta t = 1$ s and 5 s are presented in Fig. 11a and Fig. 11b, respectively. As can be seen, the prolongation of time in the MeNB is increasing with $\sigma^2(v_{inac})$. This means the scanning efficiency decreases with inaccuracy of the speed determination. This fact is more notable for shorter *GI*s. For longer *GI*s, $\sigma^2(v_{inac})$ influences the results only negligibly. Note that even low *GI* and high $\sigma^2(v_{ianc})$ cause only prolongation up to 1.5 %, which is not significant with respect to results of other algorithms (see Fig. 8). Fig. 11 also shows that even the *GI* = 1 s leads to the rapid reduction of the prolongation of the time in MeNB and nearly no prolongation occurs if the *GI* is set to 5 s disregarding accuracy in speed determination.
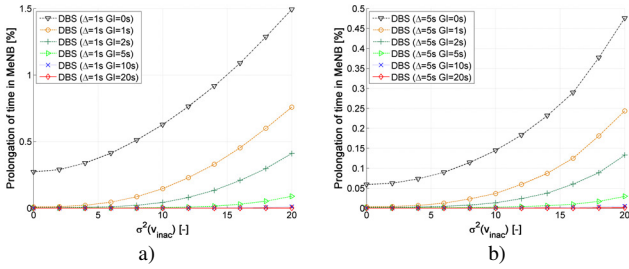

Fig. 11. Impact of variance of inaccuracy of speed determination v_{inac} on prolongation of time in MeNB ($\eta_{\Delta t}^{GI}$) for 100 SCeNBs for scanning period Δt of 1 s (a) and 5 s (b).

Fig. 11 shows that higher value of *GI* leads to earlier addition of neighboring cells to the set of scanned cells and to elimination of the problem with inaccurate determination of the speed. However, earlier scanning of neighboring cells negatively influences the energy consumption as presented in Fig. 12a for $\Delta t = 1$ s and Fig. 12b for $\Delta t = 5$ s. Both subplots of Fig. 12 lead to the conclusion that the average energy consumption rises with the *GI*. However, the difference between energy consumption for the *GI* = 0 s and *GI* = 1 s is negligible (less than 1.5 %). Even extension of the GI to 5 s increases the energy consumption only for 5 %. This impact is only marginal with respect to gains presented in Fig. 10.
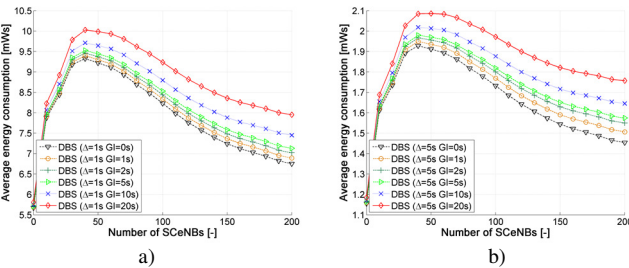

Fig. 12. Impact of GI on average energy consumption for different scanning period Δt of 1 s (a) and 5 s (b).

Based on the results in Fig. 11 and in Fig. 12, the usage of *GI* = 0 s is not recommended as it prolongs the time in MeNB while the gain in energy saving is not sufficient. On the other hand, the usage of a higher *GI* (i.e., *GI* = 10 or 20 s) leads to an increase in the energy consumption, however, at the same time, the UEs stay connected to the MeNB roughly for the same time as in case of *GI* = 5 s. Therefore, we can find a compromise between both parameters in setting the *GI* between 1 and 5 s. For these values, the impact on performance is negligible but we can eliminate even significant inaccuracy of speed determination and estimation.

VII. CONCLUSION AND FUTURE WORK

In this paper, the distance-based scanning algorithm is introduced. The proposed algorithm exploits the principle of obstructed paths and the knowledge of previous visited cell together with estimation of the relative distance between cells for selections of cells to be scanned.

As the results show, our algorithm reaches very low number of scanned cells and low energy consumption while high utilization of SCeNBs is ensured. In terms of the number of scanned cells, our proposed DBS algorithm outperforms the MSE-BS and OP algorithms for more than 90 % and 60 %, respectively. In all cases, our algorithm reaches lower energy consumption as well as higher utilization of SCeNBs then all competitive algorithms.

To avoid performance degradation of the proposed DBS algorithm due to an inaccuracy of the speed prediction, the *GI* is considered in our proposal. By using the *GI* in range of 1 and 5 seconds, the maximum utilization of SCeNBs is ensured while the energy consumption remains low even for high inaccuracy of the speed prediction.

The results shown in the paper prove that the algorithm is suitable for scenario with low as well as high density of small cells. Thus, the proposed algorithm can be used not only in existing 4G mobile networks but it is very appropriate also for future 5G heterogeneous mobile networks.

In future work, we intend to focus on self-optimization phase of the proposed algorithm in order to facilitate automatic adaptation of the set of cells for scanning if a user is attached to the MeNB to any changes in its vicinity.

REFERENCES

[1] M. Hughes and V.M. Jovanovic, "Small Cells-Effective Capacity Relief Option for Heterogeneous Networks," in *IEEE Vehicular Technology Conference 2012 (VTC Fall 2012),* Quebec, Sept. 2012.

[2] J.G. Andrews, H. Claussen, M. Dohler, S. Rangan and M.C. Reed, "Femtocells: Past, Present, and Future," *IEEE Journal on Selected Areas in Communications*, vol. 30, no. 3, pp. 497-508, Apr. 2012.

[3] 3GPP TS 36.331, "Radio Resource Control (RRC); Protocol specification," Sept. 2013.

[4] 3GPP TR 36.902, "Self–configuring and self–optimizing network (SON) use cases and solutions," Mar. 2011.

[5] 3GPP TR 25.913, "Requirements for Evolved UTRA (E–UTRA) and Evolved UTRAN (E–UTRAN)," Dec. 2009.

[6] D. Soldani and I. Ore, "Self–optimizing Neighbor Cell List for UTRA FDD Networks Using Detected Set Reporting," in *IEEE Vehicular Technology Conference 2007 (VTC Spring 2007)*, Dublin, Apr. 2007.

[7] A. Dahlen, A. Johansson, F. Gunnarsson, J. Moe, T. Rimhagen and H. Kallin, "Evaluations of LTE Automatic Neighbor Relations," in *IEEE Vehicular Technology Conference 2011 (VTC Spring 2011)*, Budapest, May 2011.

[8] P. Bhat, S. Nagata, L. Campoy, I. Berberana, T. Derham, L. Guangyi, S. Xiaodong, Z. Pingping and Y. Jin, "LTE–advanced: an operator perspective," *IEEE Communications Magazine*, vol. 50, no. 2, pp. 104-114, Feb. 2012.

This article has been accepted for publication in a future issue of this journal, but has not been fully edited. Content may change prior to final publication. Citation information: DOI 10.1109/TVT.2015.2402753, IEEE Transactions on Vehicular Technology

> REPLACE THIS LINE WITH YOUR PAPER IDENTIFICATION NUMBER (DOUBLE-CLICK HERE TO EDIT) <   12

[9] C.M. Mueller, H. Bakker and L. Ewe, "Evaluation of the Automatic Neighbor Relation Function in a Dense Urban Scenario," in *IEEE Vehicular Technology Conference 2011 (VTC Spring 2011)*, Budapest, May 2011.

[10] M. Vondra and Z. Becvar, "Self–configured Neighbor Cell List of macro cells in network with Small Cells," in *IEEE Personal Indoor and Mobile Radio Communications 2013 (PIMRC 2013)*, London, Sept. 2013.

[11] K. Han, S. Woo, D. Kang and S. Choi, "Automatic Neighboring BS List Generation Scheme for Femtocell Network," in *International Conference* on *Ubiquitous and Future Networks 2010 (ICUFN 2010)*, Jeju Island, South Korea, June 2010.

[12] M.Z. Chowdhury, T.B. Minh and M.J. Yeong, "Neighbor cell list optimization for femtocell-to-femtocell handover in dense femtocellular networks." in *International Conference* on *Ubiquitous and Future Networks 2011 (ICUFN 2011)*, Dalian, China, June 2011.

[13] 3GPP TS 36.133, "Evolved Universal Terrestrial Radio Access (E–UTRA); Requirements for support of radio resource management," Sept. 2013.

[14] A. Prasad, O. Tirkkonen, P. Lunden, O.N.C. Yilmaz, L. Dalsgaard and C. Wijting, "Energy–efficient inter–frequency small cell discovery techniques for LTE–advanced heterogeneous network deployments," *IEEE Communications Magazine*, vol. 51, no. 5, pp. 72-81, May 2013.

[15] R2-123102: Background search for small cell detection, Nokia Siemens Networks, Nokia Corporation, NTT DOCOMO, INC., TSG-RAN WG2 meeting #78, May 2012.

[16] Z. Becvar, M. Vondra and P. Mach, "Dynamic Optimization of Neighbor Cell List for Femtocells," in *IEEE Vehicular Technology Conference 2013 (VTC Spring 2013)*, Dresden, July 2013.

[17] H. Laitinen, S. Juurakko, T. Lahti, R. Korhonen and J. Lahteenmaki, "Experimental Evaluation of Location Methods Based on Signal–Strength Measurements," *IEEE Transactions on Vehicular Technology*, vol. 56, no. 1, pp. 287-296, Jan. 2007.

[18] J. Johansson, W.A. Hapsari, S. Kelley and G. Bodog, "Minimization of drive tests in 3GPP release 11," *IEEE Communications Magazine*, vol. 50, no. 11, pp. 36-43, Nov. 2012.

[19] A. Prasad, P. Lunden, O. Tirkkonen and C. Wijting, "Energy Efficient Small-Cell Discovery Using Received Signal Strength Based Radio Maps," in *IEEE Vehicular Technology Conference 2013 (VTC Spring 2013)*, Dresden, July 2013.

[20] 3GPP TR 36.839, "Evolved Universal Terrestrial Radio Access (E–UTRA); Mobility enhancements in heterogeneous networks," Dec. 2012.

[21] 3GPP TS 36.304, "Universal Terrestrial Radio Access (E–UTRA); User Equipment (UE) procedures in idle mode," Sept. 2013.

[22] W.H. Yang, Y.C. Wang, Y.C. Tseng and B.S.P. Lin, "Energy-efficient network selection with mobility pattern awareness in an integrated WiMAX and WiFi network," in *International Journal of Communication Systems*, vol. 23, no. 2, pp. 213-230, Feb. 2010.

[23] N. Kolehmainen, J. Puttonen, T. Henttonen and J. Kaikkonen, "Performance of idle mode mobility state detection schemes in Evolved UTRAN," In *IEEE International Symposium on Wireless Pervasive Computing 2010 (ISWPC 2010)*, Modena, Italy, May 2010.

[24] R2-122368: Enhanced MSE based small cell detection, Nokia Siemens Networks, Nokia Corporation, TSG-RAN WG2, May 2012.

[25] D. Soldani, G. Alford, F. Parodi and M. Kylväjä, "An Autonomic Framework for Self-Optimizing Next Generation Mobile Networks," in *IEEE World of Wireless, Mobile and Multimedia Networks 2007 (WoWMoM 2007)*, Helsinki, 2007.

[26] K.S. Hyun, E. Kim, K. Hwantae and K. Hwangnam, "Microscale Analysis on Sensing Devices and Its Impact on Assessing User Mobility," in *IEEE Advanced Information Networking and Applications 2103 (AINA 2013)*, Barcelona, Mar. 2013.

[27] B. Pricope and H. Haas, "Speed estimation for pedestrian dead-reckoning," in Proc. of the 21st IEEE International Symposium on Personal, Indoor and Mobile Radio Communications, Sept. 2010.

[28] B. Pricope and H. Haas, "Performance analysis of a novel pedestrian dead–reckoning method," in *IEEE Personal Indoor and Mobile Radio Communications 2011 (PIMRC 2011)*, Toronto, Sept. 2011.

[29] B. Pricope and H. Haas, "Experimental Validation of a New Pedestrian Speed Estimator for OFDM Systems in Indoor Environments," in *IEEE Global Telecommunications Conference 2011 (GLOBECOM 2011)*, Houston, Dec. 2011.

[30] D. Kim, B. Shin, D. Hong and J. Lim, "Self-Configuration of Neighbor Cell List Utilizing E-UTRAN NodeB Scanning in LTE Systems," in *IEEE Consumer Communications and Networking Conference 2010 (CCNC 2010)*, Las Vegas, Jan. 2010.

[31] Small Cell Forum, Interference Management in UMTS Femtocells, available online at: http://www.smallcellforum.org/smallcellforum_resources/pdfsend01.php?file=009%20Interference%20Management%20in%20UMTS%20femtocells.pdf, 2010.

[32] ITU-R P.1238-6, "Propagation data and prediction methods for the planning of indoor radio communication systems and radio local area networks in the frequency range 900 MHz to 100 GHz," 2009.

[33] T.S. Azevedo, R.L. Bezerra, C.A.V. Campos and L.F.M. De Moraes, "An Analysis of Human Mobility Using Real Traces," in *IEEE Wireless Communications and Networking Conference 2009 (WCNC 2009)*, Budapest, Apr. 2009.

[34] M. Amirijoo, P. Frenger, F. Gunnarsson, H. Kallin, J. Moe and K. Zetterberg, "Neighbor Cell Relation List and Physical Cell Identity Self-Organization in LTE," in *IEEE International Conference on Communications Workshops 2008 (ICC Workshops 2008)*, Reno, Nevada, June 2008.

Michal Vondra (M'14) received the BSc degree in electronic engineering and MSc degree in telecommunication engineering from Czech Technical University in Prague, in 2008 and in 2010, respectively. He is currently pursuing the Ph.D. degree in telecommunication engineering at Czech Technical University in Prague.

He was on internship at University College Dublin, Ireland in 2014. Since 2010, he participates in projects founded by European Commission and in several national projects. He published more than 20 conference papers, journal papers or book chapters. Currently, his research interest includes mobility management in cellular network and vehicular ad-hoc networks.

Zdenek Becvar (M'10) received the MSc and PhD degree in telecommunication engineering from the Czech Technical University in Prague, Czech Republic in 2005 and 2010, respectively. Currently, he is associate professor at the Department of Telecommunication Engineering at the same university.

From 2006 to 2007, he joined Sitronics R&D centre in Prague focusing on speech quality in VoIP. Furthermore, he was involved in research activities of Vodafone R&D center at Czech Technical University in Prague in 2009. He was on internships at Budapest Politechnic, Hungary and CEA-Leti, France in 2007 and 2013, respectively. Since 2007, he continuously participates in projects founded by European Commission. In 2013, he becomes representative of the Czech Technical University in Prague in ETSI and 3GPP standardization organizations. He is a member of more than 15 program committees at international conferences or workshops and he published 3 book chapters and more than 50 conference or journal papers. His current research interests include mobility and radio resource management in future mobile networks.